Relativistic meson spectroscopy in momentum space

H. Hersbach
Instituut voor Theoretische Fysica, Universiteit Utrecht,
Princetonplein 5, P.O. Box 80.006, 3508 TA Utrecht, The Netherlands
(Received 23 March 1994)

In this paper a relativistic constituent-quark model based on the Ruijgrok–de Groot formalism is presented. The quark model is not defined in configuration space, but in momentum space. The complete meson spectrum, with the exception of the self-conjugate light unflavored mesons, is calculated. The potential used consists of a one-gluon exchange (OGE) part and a confining part. For the confining part a relativistic generalization of the linear plus constant potential was used, which is well defined in momentum space without introducing any singularities. For the OGE part several potentials were investigated. Retardations were included at all places. By the use of a fitting procedure involving 52 well-established mesons, best results were obtained for a potential consisting of a purely vector Richardson potential and a purely scalar confining potential. Reasonable results were also obtained for a modified Richardson potential. Most meson masses, with the exception of the π, the K, and the K_0^*, were found to be quite well described by the model.

PACS number(s): 12.39.Pn, 03.65.Ge, 03.65.Pm

I. INTRODUCTION

It is generally believed that the properties of mesons and baryons should be correctly described by quantum chromodynamics (QCD). However, apart from lattice gauge calculations, a practical calculation is impossible at the moment. As a replacement simple quark models, in which hadrons are viewed as bound states of constituent quarks, are quite successful (for a review see [1]). The simplest are the nonrelativistic (NR) ones. The potential used here usually consists of a Coulomb term to account for the perturbative one-gluon exchange (OGE), and a linear potential with possibly an additional constant to incorporate the nonperturbative confining. These models work very well for the heavier charmonia and bottonia. For the lighter mesons, however, it is clear that relativistic corrections should be included. Relativistic models are most naturally formulated in momentum space. Traditionally, however, and also because of the belief that it would be impossible to describe a confining potential in momentum space, the equations are normally transformed to configuration space. Some time ago [2–7], it has been realized that there is no obstacle to define a confining potential in momentum space, even in the relativistic case. Therefore a growing interest has arisen to study quark models directly in this, to our view, more favorable representation.

This will also be the subject of this paper. A relativistic covariant quantum formalism, introduced by Ruijgrok and de Groot (RdG), will form the basis of a constituent-quark model in momentum space. The masses of all known mesons will be calculated, with the exception of the self-conjugate light unflavored ones. A proper analysis for these latter ones should allow for transitions of the form $q\bar{q} \rightarrow q'\bar{q}'$, which are not regarded in this paper.

The RdG formalism (for a review see, e.g., [8]) is defined via an as simple as possible relativistic extension of the NR Lippmann-Schwinger equation. It does not require further specification in the course of its solution and it does not start from the Bethe-Salpeter equation. The main difference is that in the intermediate states all particles remain on their mass shell, and that only total three-velocity and not four-momentum is conserved. For a two-particle system this means that in the intermediate states there are, like in the NR case, three degrees of freedom left. Therefore there is no need to make a quasipotential reduction from four to three degrees of freedom, which is a delicate point in the Bethe-Salpeter framework. For observable quantities, such as the total cross section, in addition to the conservation of total three-velocity, the total energy is conserved, so that for these physical quantities total conservation of four-momentum is restored.

Concerning the Poincaré invariance a similar situation arises as in Dirac's point form of a relativistic dynamical system [9], in which the commutation relations for the six generators of the Lorentz group $M_{\mu\nu}$ are trivially satisfied and the interaction effects must be put into the generators for the space and time translations, i.e., in the momentum operators P_μ.

The Lorentz invariance of the formalism is guaranteed, because the matrix elements $V_{\alpha\beta}$ of the potential that appears in the formalism are functions of the scalars that can be constructed out of the momenta of the individual particles. Under a space-time translation a this matrix element acquires a phase factor $e^{i(P_\alpha - P_\beta)\cdot a}$, where P_α and P_β are the total four-momenta of the initial state α and final state β. This phase factor is not equal to unity, because in the formalism the interaction does not conserve the total four-momentum. Full Poincaré invariance therefore implies that also the solution for the scattering amplitude $M_{\alpha\beta}$ in the relativized Lippmann-Schwinger equation be multiplied by the same phase factor. This situation is not different from the case of nonrelativis-

tic scattering theory: the phase factor has no observable consequences since for all measured quantities, such as the scattering cross section, the initial and final four-momentum *do* have the same value.

Negative energy states are not included in the RdG formalism. The statement that relativistic covariance requires the simultaneous existence of particles and antiparticles is correct only in the framework of a relativistic field theory, but does not apply for ordinary quantum theories, like the RdG formalism.

Retardation effects are incorporated in a simple and unambiguous way [8]. This is to be contrasted with the Bethe-Salpeter equation, where different three-dimensional quasipotential reductions lead to different retardations (see, e.g., Sec. 2.3 of [1]). In [8] it was shown that this incorporation gave rise to the correct fine-structure formulas for the hydrogen atom and positronium.

The organization of this paper is as follows. In Sec. II first a short summary of the RdG formalism will be given. The general structure of the quark-antiquark potential and its partial-wave decomposition will be considered. In Sec. III a number of quark-antiquark potentials will be discussed. A modification of the Richardson potential, to acount for the OGE, as well as a relativistic generalization of the constant potential is defined. An important feature of the mesons consisting of light quarks is the appearance of linear Regge trajectories. Their origin in the light of the present theory is discussed in Sec. IV. The numerical method used will be described in Sec. V and its results will be further discussed in Sec. VI. We end with some conclusions.

II. RESUMÉ OF THE RdG FORMALISM

In this section we will repeat the ingredients of the RdG formalism, which for the present application are most important. For a more extended review, see, e.g., [8].

A. The general framework of RdG

A state α of a quark (mass m_1) and an antiquark (mass m_2) can be characterized by $(p_1\lambda_1, p_2\lambda_2)$, where p_1 and p_2 are the four-momenta of the quark and antiquark, and λ_1 and λ_2 are their helicities. Also in intermediate states particles will remain on their mass shell, which means that $p_i^0 = \sqrt{|\mathbf{p}_i|^2 + m_i^2} \equiv E_i$, $i = 1, 2$. The formalism is constructed in such a way that in the interaction the total three-velocity is conserved. This means that the quark-antiquark potential $V_{\beta\alpha}$ for a transition from an initial state $\alpha = (p_1\lambda_1, p_2\lambda_2)$ to a final state $\beta = (p_1'\lambda_1', p_2'\lambda_2')$ contains only nonzero elements if $\mathbf{v}' = \mathbf{v}$, i.e., for which

$$\mathbf{v} = \frac{\mathbf{p}_1 + \mathbf{p}_2}{p_1^0 + p_2^0} = \frac{\mathbf{p}_1' + \mathbf{p}_2'}{p_1'^0 + p_2'^0} = \mathbf{v}'. \tag{2.1}$$

In the center-of-momentum system (cms) this velocity conservation coincides with three-momentum conservation, i.e., $\mathbf{p}_1 = -\mathbf{p}_2 \equiv \mathbf{p} \Longrightarrow \mathbf{p}_1' = -\mathbf{p}_2' \equiv \mathbf{p}'$. In this frame therefore the potential can be written as

$$V_{\beta\alpha} = V_{\lambda_1'\lambda_2',\lambda_1\lambda_2}(\mathbf{p}', \mathbf{p}).$$

In the NR case the momentum dependence of a central potential appears in the form $|\mathbf{q}|^2 = |\mathbf{p}' - \mathbf{p}|^2$. In the relativistic case this expression must be replaced by a covariant one. Here the usual replacement $|\mathbf{q}|^2 \to -q^2$ cannot be used because, due to the lack of four-momentum conservation, the loss of momentum $q_1 = p_1 - p_1'$ by the quark, will in general differ from the gain of momentum $q_2 = p_2' - p_2$ by the antiquark. Instead the following obvious and symmetrical substitution is made (see [8]):

$$|\mathbf{q}|^2 \to -q_1 \cdot q_2 = |\mathbf{p}' - \mathbf{p}|^2 - \tau(p', p), \tag{2.2}$$

where the term τ, given by

$$\tau(p', p) = (E_1 - E_1')(E_2' - E_2), \tag{2.3}$$

is responsible for retardation effects. The theoretical justification for this replacement is twofold (see [8]). In the first place it is consistent with velocity conservation. The second and more practical justification is that, in the case of the Coulomb potential, τ automatically generates the correct form for the Breit interaction (see [8]). In the equal-mass case $\tau = -(E - E')^2$, which is exactly opposite to the retardation used by Gross and Milana [4] and Maung, Kahana, and Norbury [6]. The difference in sign will give the wrong sign for the Breit interaction, which in turn will effect the fine-structure of positronium (see also the discussion given by Olsson and Miller [10]). In [8] it was shown that Eq. (2.3) gives the correct positronium fine-structure formula.

In the center-of-momentum frame (cms) the relativistic wave equation, from which the mass M of the meson is to be solved is given by ($\hbar = c = 1$)

$$[E_1 + E_2 - M]\Psi_{\lambda_1\lambda_2}(\mathbf{p}) + \sum_{\lambda_1'\lambda_2'} \int W_{\lambda_1'\lambda_2',\lambda_1\lambda_2}(\mathbf{p}', \mathbf{p})\Psi_{\lambda_1'\lambda_2'}(\mathbf{p}') \left[\frac{m_1 m_2}{E_1' E_2'}\right] d\mathbf{p}' = 0, \tag{2.4}$$

where the wave function $\Psi_{\lambda_1\lambda_2}(\mathbf{p})$ is normalized as

$$\sum_{\lambda_1\lambda_2} \int |\Psi_{\lambda_1\lambda_2}(\mathbf{p})|^2 \left[\frac{m_1 m_2}{E_1 E_2}\right] d\mathbf{p} = 1 \tag{2.5}$$

and $V = 4m_1 m_2 W$. The quantity W is introduced for convenience, because it reduces in the NR limit to the NR potential. In this limit Eq. (2.4) reduces to the NR Schrödinger equation in momentum space.

B. Decomposition

The interaction W used in the present application can be decomposed into a vector part V_V and a scalar part

V_S, which in the cms is given by

$$W(\mathbf{p}',\mathbf{p}) = \bar{u}_{\lambda_1'}(\mathbf{p}_1')\bar{v}_{\lambda_2}(\mathbf{p}_2)\left[\gamma_\mu^{(1)}\cdot\gamma^{(2)\mu}V_V(\mathbf{p}',\mathbf{p}) + \mathbb{1}^{(1)}\mathbb{1}^{(2)}V_S(\mathbf{p}',\mathbf{p})\right]v_{\lambda_2'}(\mathbf{p}_2')u_{\lambda_1}(\mathbf{p}_1). \tag{2.6}$$

Here the Dirac spinors u and v for the quark and antiquark are defined by

$$u_\lambda(\mathbf{p}) = N\begin{bmatrix}1\\ 2\lambda b\end{bmatrix}\chi(\lambda,\mathbf{p}/p),$$

$$v_\lambda(\mathbf{p}) = N\begin{bmatrix}-2\lambda b\\ 1\end{bmatrix}(-i)\sigma_2\chi^*(\lambda,\mathbf{p}/p),$$

with $N = \sqrt{(E+m)/(2m)}$, $b = p/(E+m)$, and $\chi(\lambda,\mathbf{p}/p)$ the helicity spinor with helicity λ. For the two-particle helicity states we use the conventions introduced by Jacob and Wick [11]. Potential Eq. (2.6) partially decouples with respect to the states $|p;JM;\lambda_1\lambda_2\rangle$, which are defined by (18) of [11], giving

$$\langle p';J'M';\lambda_1'\lambda_2'|W|p;JM;\lambda_1\lambda_2\rangle = \delta_{JJ'}\delta_{MM'}\langle\lambda_1'\lambda_2'|W^J(p',p)|\lambda_1\lambda_2\rangle. \tag{2.7}$$

The determination of this decoupling is a technical matter. In [12] this calculation was given in detail for the case in which only one of the two particles carries spin. For the present case of both particles carrying spin, an analogous analysis can be made. This analysis, however, is much more complex and therefore we will only give the result of the reduction.

Because of conservation of parity, W further decomposes into two 2×2 submatrices, each having a definite parity. The subspace spanned by

$$|t_1\rangle = \frac{1}{\sqrt{2}}[|\tfrac{1}{2},\tfrac{1}{2}\rangle + |-\tfrac{1}{2},-\tfrac{1}{2}\rangle],$$

$$|t_2\rangle = \frac{1}{\sqrt{2}}[|\tfrac{1}{2},-\tfrac{1}{2}\rangle + |-\tfrac{1}{2},\tfrac{1}{2}\rangle] \tag{2.8}$$

has parity $(-1)^{J+1}$. It contains the triplet $J = l\pm 1$ states. The complementary subspace, spanned by

$$|s_1\rangle = \frac{1}{\sqrt{2}}[|\tfrac{1}{2},\tfrac{1}{2}\rangle - |-\tfrac{1}{2},-\tfrac{1}{2}\rangle],$$

$$|s_2\rangle = \frac{1}{\sqrt{2}}[|\tfrac{1}{2},-\tfrac{1}{2}\rangle - |-\tfrac{1}{2},\tfrac{1}{2}\rangle], \tag{2.9}$$

has parity $(-1)^J$ and contains the $J = l$ singlet and triplet states. Only in the equal-mass case does this subspace further split into two 1×1 subspaces. Let

$$V_{ij}^{nJ} = p'p\frac{m_1m_2}{\sqrt{E_1'E_2'E_1E_2}}\langle n_i|W^J(p',p)|n_j\rangle,\quad n = s,t, \tag{2.10}$$

then the eigenvalue equation (2.4) can be cast in the form (by suppressing the quantum numbers J, M, and s or t)

$$[E_1+E_2-M]\,f_i(p) + \sum_j\int_0^\infty V_{ij}(p',p)f_j(p')dp' = 0. \tag{2.11}$$

In Appendix A explicit formulas for $V_{ij}^{nJ} = (V_V)_{ij}^{nJ} + (V_S)_{ij}^{nJ}$ are given. The reduced wave function f is normalized to

$$\sum_i\int_0^\infty |f_i(p)|^2dp = 1. \tag{2.12}$$

C. Quantum numbers

For a potential of the form Eq. (2.6) the total angular momentum J and the parity P are conserved quantities. In a relativistic theory involving particles carrying spin, the orbital angular momentum is not conserved and is therefore not a good quantum number. If the relativistic effects are not too large, however, l is still approximately conserved. Therefore l is often regarded as an "almost good" quantum number (for a discussion see, e.g., [13]). For convenience the number l can still be used to distinguish between different states. Examples of this are the $J = l\pm 1$ triplet states. Only in the NR case are these states actual eigenstates, in the relativistic case they will in principle mix.

For the self-conjugate mesons there is an additional conserved quantum number: charge conjugation C. Indeed it was seen in the previous subsection, that for this equal-mass case the channel containing the $J = l$ singlet and $J = l$ triplet decouples. Both the charge conjugation C and the parity P can be expressed in terms of the total spin $S^2 = s(s+1)$ ($s = 0$ for singlet, $s = 1$ for triplet states) and l:

$$P = (-1)^{l+1}\ \text{ and }\ C = (-1)^{l+s}. \tag{2.13}$$

Also s is not a good quantum number, but can like l still be used to label states.

III. THE QUARK-ANTIQUARK POTENTIAL

The quark-antiquark potential must contain a one-gluon exchange (OGE) to account for the short range, and a confining part for the long range interaction. It

is generally believed that $V_{\rm OGE}$ should have a vector Lorentz structure, because this follows from the QCD Lagrangian. About the confining part $V_{\rm con}$ there is no such consensus (see, e.g., [1]). Some believe that it must have a purely scalar structure, while others admit a mixture between scalar and vector coupling. We will adopt this last point of view. The potential can therefore be written in the form [see Eq. (2.6)]

$$\begin{aligned} V_V &= V_{\rm OGE} + \epsilon V_{\rm con}, \\ V_S &= (1-\epsilon) V_{\rm con}, \end{aligned} \tag{3.1}$$

where ϵ represents the scalar-vector mixing of the confining potential.

For $V_{\rm con}$ the relativistic generalization of the linear potential, as described in [7], plus a constant potential (to be defined in Sec. III B) was used. This generalization is defined in a formal way and does not introduce any singularities. For the OGE two different potentials were used: the Richardson potential [14] and a modified version of this potential (to be defined in Sec. III A), both containing a running coupling constant (see Sec. III A). The Richardson potential contains a linear part by itself. Therefore in this case (from now on denoted by case I), $\epsilon = 0$ was chosen, so that the confining in the vector direction is completely determined by the Richardson potential. The modified Richardson potential has no linear part. Therefore in this case (denoted by case II) a nonzero ϵ was admitted.

In all these potentials the NR momentum transfer $|\mathbf{q}|^2$ is replaced by $-q_1 \cdot q_2$ [see Eq. (2.2)] and it is this replacement that ensures the inclusion of retardation effects at all places. For notational convenience, the quantity

$$Q \equiv \sqrt{-q_1 \cdot q_2} \tag{3.2}$$

is introduced. In the NR limit it reduces to $|\mathbf{q}|$.

A. The one-gluon exchange: Running coupling constant

The renormalization scheme of perturbative QCD says that, for large momentum transfer, the running coupling constant α_s in

$$V_{\rm OGE} = -\frac{4}{3}\frac{\alpha_s(Q^2)}{2\pi^2 Q^2} \tag{3.3}$$

is given by (see also (B2) of [24])

$$\alpha_s(Q^2) = \frac{a_n}{X_n}\left[1 - b_n \frac{\ln(X_n)}{X_n} + \mathcal{O}\left(\frac{\ln^2(X_n)}{X_n^2}\right)\right]. \tag{3.4}$$

The factor $\frac{4}{3}$ arises from color averaging. In Eq. (3.4)

$$a_n = \frac{12\pi}{(33-2n)}, \qquad b_n = \frac{6(153-19n)}{(33-2n)^2},$$

$$X_n = \ln\left[Q/\Lambda_{\overline{\rm MS}}^{(n)}\right]^2$$

and n is the number of quarks with a mass smaller than Q. The subscript $\overline{\rm MS}$ denotes that the renormalization is performed according to the modified minimal subtraction scheme. The connection between the different $\Lambda_{\overline{\rm MS}}^{(n)}$'s is given by (B4) of [24]. The typical momentum transfer within a meson is on the order of 1 GeV, so in this region $n = 3$. Therefore, Eq. (3.4) with $n = 3$ is in many cases used as an approximation for all large momentum transfers. In addition, the b_3 term is almost always neglected. But this term is not small at all: in the Q region from 1 to 5 GeV its contribution is about 25%. Even for very high momentum transfers its contribution is substantial $\sim 15\%$ for $Q = 50$ GeV. However, it appears that when $\Lambda_{\overline{\rm MS}}^{(5)}$ rather than $\Lambda_{\overline{\rm MS}}^{(3)}$ is used, a fairly good approximation of Eq. (3.4) for large Q is obtained by putting

$$\alpha_s \approx \frac{a_3}{X_5} \tag{3.5}$$

(see the curve "standard approximation" of Fig. 1). For $Q = 5$ GeV the deviation from Eq. (3.4) is $\sim 7\%$, and for $Q \sim 50$ GeV there is no detectable difference. Also for smaller Q the agreement is better, but of course in this region the validity of Eq. (3.4) is doubtful. Nevertheless, we think that these considerations show that there is no theoretical necessity to stick to the value of a_3 in Eq. (3.5): a small deviation from it also results in a good running coupling constant for large Q. We will use this freedom for the two OGE potentials discussed in the remainder of this subsection.

For small positive Q values Eqs. (3.4) and (3.5) diverge. To remedy this, Richardson [14] proposed a potential in which the divergence is shifted to the origin by making the replacement $Q^2 \to Q^2 + \Lambda^2$ in Eq. (3.5):

$$\begin{aligned} V_R(Q^2) &= -\frac{\alpha_0}{2\pi^2 Q^2 \ln[1 + \frac{Q^2}{\Lambda^2}]} \\ &= -\frac{\alpha_0 \Lambda^2}{2\pi^2 Q^4} - \frac{\alpha_0}{4\pi^2 Q^2} + \cdots \quad \text{for } Q \to 0. \end{aligned} \tag{3.6}$$

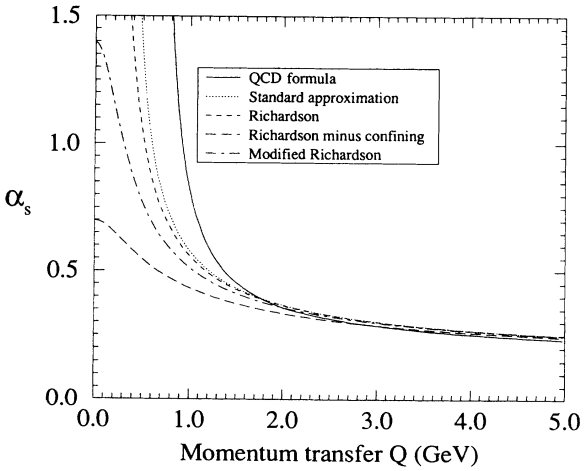

FIG. 1. Running coupling constant $\alpha_s(Q^2)$, defined by (3.3) for three different choices of $V_{\rm OGE}$ compared to the QCD formula (3.4) and its standard approximation (3.5). $\Lambda = \Lambda_{\overline{\rm MS}}^{(5)} = 0.3$ GeV and $\alpha_0 = 16\pi/27$.

The color factor $\frac{4}{3}$ is absorbed in α_0. In Fig. 1 the running coupling constant, defined via Eq. (3.3) with $V_{\rm con} = V_R$, is compared to the QCD formula for $\alpha_0 = \frac{4}{3}a_3 = 16\pi/27 = 1.862$. The singularity for $Q = 0$ results from a linear term in the potential with string tension $\frac{1}{2}\alpha_0\Lambda^2$ (see [7]). When the singularity is subtracted, the running coupling constant saturates to the value $\frac{1}{2}a_3 = 0.698$. From Fig. 1 it is seen that for momentum transfers starting from 2 GeV, a much better approximation to Eq. (3.4) is obtained, if α_0 is slightly decreased. A value of $\alpha_0 = 1.750$ turns out to be a very good choice.

A different way to remove the singularities is to also make the replacement $Q^2 \to Q^2 + \Lambda^2$ in $1/Q^2$ itself. This results into

$$V_M(Q^2) = -\frac{\alpha_0}{2\pi^2[Q^2+\Lambda^2]\ln[1+\frac{Q^2}{\Lambda^2}]} = -\frac{\alpha_0}{2\pi^2 Q^2} + \cdots \quad \text{for } Q \to 0. \tag{3.7}$$

This modified Richardson potential V_M does not contain a linear part. The coupling constant saturates to a value a_3. The running coupling constant defined via this potential is given in Fig. 1 for $\alpha_0 = \frac{4}{3}a_3$. From this figure it is seen that this choice for α_0 gives a good representation of the QCD formula for moderate Q values.

The spinless partial waves W_R and W_M of V_R and V_M, defined by Eq. (A1), are given in Appendix B.

B. The confining: "Linear + constant" potential

For the confinement a relativistic generalization of a linear plus constant potential was used:

$$V_{\rm con} = V_{\rm lin} + V_{\rm C}. \tag{3.8}$$

As was also discussed in [7], it was for a long time believed that a linear potential could not correctly be described in momentum space. A naive consideration shows that it behaves like $-1/Q^4$, which results in an ill-defined bound-state equation. A few years ago it was shown [2,3,5] that this singularity for the NR case is only apparent. For the relativistic case different methods were employed [4,6,7] to solve this problem. In this paper we use the definition given in [7]:

$$V_{\rm lin} = \lim_{\eta\downarrow 0} \frac{\partial^2}{\partial\eta^2}\frac{\lambda}{2\pi^2}\left[\frac{1}{Q^2+\eta^2}\right], \tag{3.9}$$

where λ is the string tension. It was shown in [7] that the limit exists in a distributional sense. The result was that the integral in Eq. (2.11) is replaced by

$$\int_0^\infty \left[V_{ij}^{(nJ)}(p',p)f_j(p') + \frac{4p^2 C_{ij}(p)}{(p'^2-p^2)^2}f_j(p)\right]dp'. \tag{3.10}$$

Here V_{ij}^{nJ}, $n = s,t$, is the naive pointwise limit obtained from Eq. (3.9). The $1/(p'-p)^2$ singularity it contains is removed by the quantity

$$C_{ij}(p) = \lim_{p'\to p}\left[-[p'-p]^2 V_{ij}^{(nJ)}(p',p)\right]. \tag{3.11}$$

The resulting $1/(p'-p)$ singularity is handled by the principal-value integral (denoted by $\mathcal{f}$). It was shown that this subtraction is not just a trick to avoid singularities, but is in fact generated by definition Eq. (3.9).

For a confining potential which consists of a mixture of a scalar and vector Lorentz structure [see Eq. (3.1)], the pointwise limits of the spinless partial waves [see Eq. (A1)] are given by $W_V^l = \epsilon W_L^l$ and $W_S^l = (1-\epsilon)W_L^l$, where

$$W_L^l(p',p) = \frac{\lambda}{\pi}R(p',p)\frac{Q_l'(z_0)}{p'p} \tag{3.12}$$

and also $R(p',p)$ is given in Appendix A. Here z_0 is defined by Eq. (B2) and Q_l is the Legendre function of the second kind of order l. The $1/(p'-p)^2$ singularity of W_L^l is determined by

$$-\frac{\lambda}{\pi}\frac{R(p,p)}{(p'-p)^2 - \tau(p',p)}.$$

The retardation defined by Eq. (2.3) behaves around $p' \approx p$ like

$$\tau(p',p) = -\frac{p^2}{E_1E_2}(p'-p)^2 + \cdots$$

and therefore contributes to the singularity. If one combines limit equations (3.11) and (3.12) with the results of Appendix A, it can be shown that C_{ij} is given by

$$C_{ij}(p) = \frac{\lambda}{\pi}\left[\epsilon + (1-\epsilon)\frac{m_1m_2}{p_1\cdot p_2}\right]\delta_{ij}, \tag{3.13}$$

where $p_1\cdot p_2 = E_1E_2 + |\mathbf{p}|^2$ is the dot product between the four-vectors p_1 and p_2. Note that C_{ij} does not depend on J and the parity s or t. In addition it is a manifest Lorentz covariant quantity.

When the interaction does not contain a linear part, the integral Eq. (3.10) coincides with the integral in Eq. (2.11). This is so because then $C_{ij} = 0$ and there is no $1/(p'-p)$ singularity, which means that the principal value coincides with an ordinary integral. Therefore the replacement equation (3.10) in combination with Eq. (3.11) can be applied to the entire interaction. In this way a nonzero value of C automatically indicates the presence of a linear term. For the Richardson potential Eq. (3.6) with a purely vector character results in

$$(C_R)_{ij} = \frac{\alpha_0\Lambda^2}{2\pi}\delta_{ij}, \tag{3.14}$$

which indeed indicates a linear term with string tension $\frac{1}{2}\alpha_0\Lambda^2$.

In analogy with the linear potential the constant potential V_C can also be defined via the Yukawa potential. In the NR case one has in configuration space

$$V_C(r) = C = \lim_{\eta\downarrow 0}\frac{\partial}{\partial\eta}\left[-\frac{Ce^{-\eta r}}{r}\right].$$

Therefore in momentum space an obvious relativistic generalization is

$$V_C(Q^2) = \lim_{\eta \downarrow 0} \frac{\partial}{\partial \eta} \left[-\frac{C}{2\pi^2(Q^2+\eta^2)} \right]. \tag{3.15}$$

Note that this expression also includes retardations, which are hidden in Q^2 [see Eq. (3.2)]. The definition, Eq. (3.15), has to be included in the integral of Eq. (2.11) before the limit is taken. The spinless partial wave W_η^l of this constant potential is given by

$$W_\eta^l(p',p) = -\frac{CR(p',p)}{\pi} \frac{\eta}{p'p} Q_l' \left[z_0 + \frac{\eta^2}{2p'p} \right].$$

The only term that survives the limit $\eta \downarrow 0$ is

$$\frac{CR}{\pi} \frac{\eta}{(p'-p)^2 - \tau + \eta^2} \to CR \left[\frac{E_1 E_2}{p_1 \cdot p_2} \right]^{\frac{1}{2}} \delta(p'-p) + \cdots.$$

For a confining potential that has both a scalar and vector part [see Eq. (2.6)] this results in

$$(V_C)_{ij}^{nJ} = C \left[\frac{p_1 \cdot p_2}{E_1 E_2} \right]^{\frac{1}{2}} \left(\epsilon + (1-\epsilon) \frac{m_1 m_2}{p_1 \cdot p_2} \right) \delta(p'-p) \delta_{ij}. \tag{3.16}$$

IV. LINEAR REGGE TRAJECTORIES

Experimentally it is found that the mesons which consist of the light u, d, and s quarks only, lie on so-called linear Regge trajectories. This means that there are several groups of mesons, for which the mass squared for each meson within such a group is proportional to its angular momentum J, i.e., $M_J^2 \approx \beta J + C$. The constant C depends on the group, the Regge slope β however is about the same for all groups. Its experimental value is $\beta \approx 1.2$ GeV^2. For mesons containing a heavy c or b quark, such trajectories have not been observed. This suggests that linear trajectories are induced by relativistic effects. In fact, it is known [1,15,16], that the Schrödinger equation with ultrarelativistic (UR) kinematics (i.e., $2p$ instead of $p^2/2\mu$) for a linear potential, does indeed give rise to linear trajectories, while the (NR) Schrödinger equation does not. The slope β is in such a case found to depend only on the string tension λ, namely $\beta = 8\lambda$.

For the present case a similar effect is observed. It numerically appears that the UR limit (i.e., $m_1, m_2 \to 0$) of the bound-state equation, Eq. (2.11), also leads to linear trajectories, with a group-independent slope β. This slope, however, depends on the vector part λ_V of the string tension only. It is found to be a factor $\sqrt{2}$ larger than for the relativized Schrödinger equation, namely

$$\beta \approx (8\sqrt{2})\lambda_V. \tag{4.1}$$

This dominance of the vector part was also observed by Tiemeijer and Tjon [17,18], who studied a quark model based on the Bethe-Salpeter equation in configuration space. In addition they found [19,18] that the confining in the vector direction should not exceed a certain value, because then, due to the negative energy states, unphysical solutions would arise. This critical behavior which, as Tiemeijer and Tjon explain, is similar to the Klein paradox for the Dirac equation, and is related to the creation of an unbound number of quark-antiquark pairs. This breakdown does not occur for the present work, for the simple reason that it does not contain negative-energy states.

As can be deduced from Appendix A , the off-diagonal elements V_{12} and V_{21} of both a vector and a scalar potential vanish in the UR limit. Therefore Eq. (2.11) further decouples into two single equations. For the pure vector case, it reduces for the V_{11}^{tJ} channel to

$$[2p - M] f_J(p) + \int_0^\infty \left[V^J(p',p) f_J(p') + \frac{\lambda}{\pi} \frac{4p^2}{(p'^2 - p^2)^2} f_J(p) \right] dp' = 0, \tag{4.2}$$

with

$$V^J(p',p) = \frac{2\lambda}{\pi p'p} Q_J' \left[\frac{p'^2 + p^2 + (p'-p)^2}{2p'p} \right]. \tag{4.3}$$

This equation was solved numerically using the method described in Sec. V. The calculated masses (in units of $\sqrt{\lambda}$) of the lowest states for each J are presented in Table I. The Schrödinger equation with UR dynamics is in momentum space also given by Eq. (4.2), but now with

$$V^J(p',p) = \frac{\lambda}{\pi p'p} Q_J' \left[\frac{p'^2 + p^2}{2p'p} \right]. \tag{4.4}$$

The corresponding calculated masses are also listed in Table I. They all agree with the calculations performed by Basdevant and Boukraa (see Table I of [15]).

In principle the trajectories are expected to be linear only for large values of J. However, as Table I shows, the convergence is very fast. It was found that also for moderate masses Eq. (2.11) leads to Regge trajectories with the same relation, Eq. (4.1), between β and λ. The convergence, however, is then slower. When in addition a OGE term and a constant are added to the potential, the relation, Eq. (4.1), is affected. The change, however, is not very large. Therefore it can be concluded that, in order to obtain reasonable Regge slopes, the string tension in the vector direction λ_V should be around $\lambda_V \approx 0.1$ GeV^2.

TABLE I. Regge trajectories calculated from the ultrarelativistic (4.2). The masses are expressed in terms of $\sqrt{\lambda}$, where λ is the string tension.

	Present case potential (4.3)		Basdevant and Boukra [15] potential (4.4)	
J	M_J	$(M_J^2 - M_{J-1}^2)/(8\sqrt{2})$	M_J	$(M_J^2 - M_{J-1}^2)/8$
0	3.830		3.157	
1	5.062	0.969	4.225	0.985
2	6.066	0.987	5.079	0.994
3	6.931	0.993	5.811	0.996
4	7.701	0.996	6.461	0.998
5	8.402	0.998	7.052	0.999
6	9.049	0.998	7.597	0.998

V. NUMERICAL METHOD

The present model is defined by the eigenvalue equation, Eq. (2.4), in combination with a quark-antiquark potential W consisting of a one-gluon exchange part $V_{\rm OGE}$ and a confining part $V_{\rm con}$. The way in which $V_{\rm OGE}$ and $V_{\rm con}$ enter in the eigenvalue equation, Eq. (2.4), is given by Eqs. (2.6) and (3.1). The OGE potential (see Sec. III A) is determined by two parameters α_0 and Λ and the confining potential (see Sec. III B) is determined by a string tension λ and a constant C. Furthermore, a parameter ϵ can be introduced to give the confining potential a mixed scalar-vector character.

The numerical solution of the model can be divided into two parts. The first one concerns the calculation of the masses of the mesons, from the eigenvalue equation, Eq. (2.11), given all parameters of the potential under consideration, and the quark masses. The second part is the fitting to the experimental data. The eigenvalue equation was solved by expanding the wave function into cubic Hermite splines (see [20]). The integration region $p \in [0, \infty)$ was projected onto the finite interval $x \in [0, 1]$ by $x = (p-p_0)/(p+p_0)$, where p_0 was chosen in the physical region. On this interval N equidistant spline intervals were chosen on which $2N$ spline functions were defined. The matrix elements of the resulting eigenvalue equation for the expansion coefficients only involved single integrations of the potential times a spline function. This is a major advantage of the spline method compared to the more conventional expansion techniques, where the evaluation of matrix elements involves two-dimensional integrals. The integration was performed using Gauss-Legendre quadratures. In the case where the singular point $p' = p$ was inside the region of integration, special care had to be taken. In the first place, an even number of abscissas centered around $p' = p$ was used. In that way the principal value, which occurs for the confining potential, is automatically taken care of [5,21]. Second, the logarithmic singularity $\sim \ln(|p' - p|)$, which is induced by both the Coulomb and the confining potential, was separately handled by means of Gaussian quadratures based on a logarithmic weight function (see e.g., Table 25.7 of [22]). Another important advantage of using Hermite splines is their small nonzero domains. Therefore on each spline interval only a few of these splines (four for the Legendre and three for the logarithmic quadrature) were needed to obtain high accuracies. The matrix equation was solved using standard techniques [23], giving the meson masses M_i.

The choice of the projection parameter p_0 and the number of intervals N, depended on the specific meson. For instance, the typical momentum transfer for the Υ mesons ($b\bar{b}$) is about 1 GeV, so $p_0 = 1$ GeV. The masses of these mesons are all known to a high precision and they are all radial levels of the $J^{\rm PC} = 1^{--}$ channel. The Υ^v is the tenth radial state ($n = 10$). Therefore 20 spline intervals were needed to guarantee accurate results. The K_2^*, however, is the only known $J^P = 2^+$ strange meson, apart from the unconfirmed $K_2^{*\prime}$. Therefore $N = 8$ was sufficient to obtain reliable results. $p_0 = 0.5$ GeV was a proper choice for this meson.

The second part of the problem was to get a good fit to the experimental data. For this purpose the merit function

$$\chi^2(a_1, \ldots, a_n) = \sum_i \left[\frac{M_i^{\rm the}(a_1, \ldots, a_n) - M_i^{\rm expt}}{\sigma_i} \right]^2 \tag{5.1}$$

has to be optimized with respect to the parameters $a_1, \ldots, a_n$. Here i labels the mesons, $M_i^{\rm expt}$ and $M_i^{\rm the}$ denote their experimental and calculated masses, and σ_i their weights. A nonlinear regression method, based on the Levenberg-Marquardt algorithm was used to perform the fits (see Sec. 15.5 of [23]). This method requires as input the explicit knowledge of the derivatives of the calculated masses with respect to the fit parameters. For the present complex situation this information is not known. It is only known that the derivatives of a meson mass with respect to quark masses it does not contain, is equal to zero. Therefore the derivatives were approximated in the least time consuming way by the following expression:

$$\frac{\partial M_i^{\rm the}}{\partial a_j} \approx \frac{M_i^{\rm the}(a_1, \ldots, a_j + \Delta, \ldots, a_n) - M_i^{\rm the}(a_1, \ldots, a_n)}{\Delta}. \tag{5.2}$$

In this manner all required information, i.e., $M_i^{\rm the}$ and $\partial M_i^{\rm the}/\partial a_j$, is obtained by calculating all meson masses

$(n+1)$ times. A more sophisticated method would considerably increase this number. The approximation, Eq. (5.2), turned out to be very effective: starting with a physically sensible set of parameters, after four or five steps convergence to an optimum was reached. The value of the parameter Δ appeared to be of minor importance. $\Delta = 0.04$ (dimensionless, in GeV, or GeV^2, depending on the dimension of a_j) was found to be a good choice.

All mesons regarded to be established by the 1992 Particle Data Group [24] (in Table III indicated by a "•") were used in the fit, with the exception of the self-conjugate light unflavored ones. For a fair description of these mesons, an annihilation interaction from initial $q\bar{q}$ states to final $q'\bar{q}'$ states should be included. Also the charmed strange D_s^* and D_{sJ} were excluded, because of the uncertainty of their quantum numbers. Furthermore the up and down quarks were considered to be of equal mass. In addition the electromagnetic interactions are completely neglected. Therefore the π^0 and $\pi^\pm$, the K^0 and $K^\pm$, and so on will be degenerate in this picture. Because of the indistinguishability of the u and d quarks, from now on such a quark will be denoted by "u/d." This accumulates to a total of 52 mesons: 11 light unflavored ($u/d\bar{u}/\bar{d}$), 11 strange ($s\bar{u}/\bar{d}$), 4 charmed ($c\bar{u}/\bar{d}$), 2 charmed strange ($c\bar{s}$), 10 charmonia ($c\bar{c}$), 2 bottom ($b\bar{u}/\bar{d}$), and 12 bottonia ($b\bar{b}$).

For the weight σ_i the maximum of the uncertainty dM_i^{expt} of the measured mass and the predictive power of the model, was taken. It is difficult to give an estimate for this predictive power. In the first place quark models have a phenomenological nature; there is no direct link with QCD. In the second place, most mesons are in fact resonances. The decay mechanisms, which are not incorporated in this paper, could considerably effect the position of the calculated masses. This especially applies for the mesons that have decay widths of a few hundred MeV. To account for all of this, a grid size $S = 20$ MeV was introduced to give a minimum to σ. Only for bottonium ($b\bar{b}$), a grid size of 10 MeV was used, because in this system relativistic effects are less important and most states have narrow widths. Summarizing, the weights were determined by the following formula

$$\sigma_i = \text{Max}\left[dM_i^{\text{expt}}, S\right]. \tag{5.3}$$

A few exceptions to this rule were made. The pion π and the kaon K are the ground states of the $u/d\bar{u}/\bar{d}$ and $s\bar{u}/\bar{d}$ mesons, respectively. It is commonly believed that in order to give a fair description of these particles the mechanism of chiral symmetry breaking should be included in the model. It appeared that also the K_0^* mass was badly described by the model. This state, however, has a large decay width of ~ 300 MeV. Therefore $\sigma_\pi = 0.4$ GeV and $\sigma_K = \sigma_{K_0^*} = 0.2$ GeV were chosen, so that these states get an insignificant weight in the fit. Another point are the ρ' and ρ''. These states also have large decay widths ($\sim$ 300 MeV). It appeared that best results were obtained if each state was regarded to be composed of two neighboring resonances. In Sec. VI this point will be discussed in more detail.

To decrease the computation time first a rough fit was made by taking only half of the spline intervals N needed to obtain the desired accuracies. The resulting fit parameters were then used as the starting point for a full accuracy fit. The typical computation time for a complete rough fit for all 52 mesons was 30 min on a Sparc 2 workstation, while the fine tuning fit took about 1 h.

As was already mentioned, two different types of potentials were examined. In case I the Richardson potential V_R was taken to account for the OGE and for the confinement in the vector direction. V_{con} has a purely scalar character ($\epsilon = 0$). For α_0 both the "QCD" value $16\pi/27$ and the value 1.75, which gives a better agreement with the QCD formula, Eq. (3.4), were taken. Both choices ended in comparable fits ($\chi^2 \approx 260$). The resulting parameters for $\alpha_0 = 1.75$ (denoted by Ia) are given in Table II and the calculated meson spectrum in Table III. Also the case in which neither α_0 nor ϵ was fixed was regarded. The regression method led to very small values for ϵ and the string tension λ. Therefore a fit, denoted by Ib, was made where these two parameters were put equal to zero, and where α_0 was varied. This resulted in a somewhat better fit (Ib) with $\chi^2 = 250$ (see also Tables II and III). In both cases seven parameters, three to model the potential and four quark masses, were fit. Finally, the case was considered in which the linear term of V_R was subtracted. To get a confining potential in the vector direction, the mixing ϵ was also varied. This choice is very similar to the quark-antiquark potential used by Crater and Alstine [25]. The results did not

TABLE II. Final parameter sets from the fitting procedure described in Sec. V for potential models I and II. The varied parameters are indicated by a "•." For model I two different fits were made. In case Ia α_0 was held fixed and λ was fitted, while in case Ib λ was put equal to 0 and α_0 was fitted. The related quantities are discussed in Sec. VI.

Model:	Ia	Ib	II
Potential			
V_{OGE}	V_R (3.6)	V_R (3.6)	V_M (3.7)
V_{con}	$V_{\text{lin}} + V_C$	$V_{\text{lin}} + V_C$	$V_{\text{lin}} + V_C$
Parameters			
α_0	1.750	2.434 •	1.862
Λ (GeV)	0.324 •	0.320 •	0.376 •
λ (GeV^2)	0.077 •	0	0.136 •
C (GeV)	-1.297 •	-1.291 •	-1.038 •
ϵ	0	0	0.523 •
Quark masses			
$m_{u/d}$ (GeV)	0.512 •	0.699 •	0.966 •
m_s (GeV)	0.766 •	0.889 •	1.072 •
m_c (GeV)	2.066 •	2.206 •	2.249 •
m_b (GeV)	5.474 •	5.616 •	5.593 •
# parameters	7	7	8
χ^2	263	250	322
Related quantities			
λ_{tot} (GeV^2)	0.169	0.125	0.136
β (GeV^2)	1.18±0.05	1.27±0.09	0.93±0.08
ρ	0.81	0.79	0.75
α_s(34 GeV)	0.141	0.196	0.155
$\alpha_s(M_Z = 91$ GeV)	0.1164	0.161	0.127

TABLE III. Meson spectrum calculated from (2.11) for three different parameter sets Ia, Ib, and II, (see Table II). All masses are in GeV. The experimental values are taken from [24], with the exception of the h_{c1}, which is taken from [28]. The mesons labeled with a "•" (regarded as being established by [24]) were, with the exclusion of the D_s^* and the D_{sJ}, involved in the fitting procedure. The weights σ_i are determined by (5.3). The most dominant $^{2s+1}L_J$ waves are in bold.

	Name i	J^{PC}	$^{2s+1}L_J$	$M_i^{\rm expt}$	n	$M_i^{\rm Ia}$	$M_i^{\rm Ib}$	$M_i^{\rm II}$	σ_i
			Light unflavored mesons: u/d quarks						
•	π	0^{-+}	$^1S_0$	0.135	1	0.600	0.595	0.688	0.400
•	π'	0^{-+}	$^1S_0$	1.300	2	1.243	1.206	1.292	0.100
	π''	0^{-+}	$^1S_0$	1.775	3	1.711	1.671	1.695	
•	ρ	1^{--}	$^3\mathbf{S}_1/^3D_1$	0.768	1	0.754	0.762	0.867	0.020
		1^{--}	$^3\mathbf{S}_1/^3D_1$		2	1.365	1.345	1.387	
•	ρ'	1^{--}	$^3S_1/^3\mathbf{D}_1$	1.465	3	1.474	1.477	1.460	0.025
•	ρ''	1^{--}	$^3\mathbf{S}_1/^3D_1$	1.700	4	1.806	1.786	1.764	0.020
		1^{--}	$^3S_1/^3\mathbf{D}_1$		5	1.865	1.864	1.807	
	ρ'''	1^{--}	$^3\mathbf{S}_1/^3D_1$	2.100	6	2.162	2.151	2.065	
	ρ^{iv}	1^{--}	$^3S_1/^3\mathbf{D}_1$	2.150	7	2.200	2.206	2.096	
•	a_0	0^{++}	$^3P_0$	0.983	1	1.012	0.981	1.017	0.020
	a_0'	0^{++}	$^3P_0$	1.320	2	1.517	1.464	1.510	
•	a_1	1^{++}	$^3P_1$	1.260	1	1.166	1.163	1.197	0.030
•	a_2	2^{++}	$^3\mathbf{P}_2/^3\mathbf{F}_2$	1.318	1	1.301	1.319	1.329	0.020
	COG		$^3P_{0,1,2}$	1.262	1	1.224	1.229	1.250	
•	b_1	1^{+-}	$^1P_1$	1.232	1	1.183	1.194	1.231	0.020
•	π_2	2^{-+}	$^1D_2$	1.670	1	1.590	1.614	1.561	0.020
	π_2'	2^{-+}	$^1D_2$	2.100	2	1.958	1.986	1.880	
•	ρ_3	3^{--}	$^3\mathbf{D}_3/^3G_3$	1.691	1	1.698	1.734	1.637	0.020
	ρ_3'	3^{--}	$^3\mathbf{D}_3/^3G_3$	2.250	2	2.051	2.092	1.940	
		3^{--}	$^3D_3/^3\mathbf{G}_3$		3	2.097	2.152	1.969	
	a_3	3^{++}	$^3\mathbf{F}_3$	2.050	1	1.915	1.957	1.813	
	a_4	4^{++}	$^3\mathbf{F}_4/^3H$	2.040	1	2.021	2.085	1.883	
	ρ_5	5^{--}	$^3\mathbf{G}_5/^3I_5$	2.350	1	2.297	2.395	2.093	
	a_6	6^{++}	$^3\mathbf{H}_6/^3J_6$	2.450	1	2.540	2.677	2.279	
			Strange mesons (Kaons): s, u/d quarks						
	Name i	J^{PC}	$^{2s+1}L_J$	$M_i^{\rm expt}$	n	$M_i^{\rm Ia}$	$M_i^{\rm Ib}$	$M_i^{\rm II}$	σ_i
•	K	0^-	$^1S_0$	0.495	1	0.762	0.723	0.781	0.200
	K'	0^-	$^1S_0$	1.460	2	1.402	1.329	1.385	
	K''	0^-	$^1S_0$	1.830	3	1.864	1.786	1.786	
•	K^*	1^-	$^3\mathbf{S}_1/^3D_1$	0.894	1	0.891	0.876	0.955	0.020
•	$K^{*\prime}$	1^-	$^3\mathbf{S}_1/^3D_1$	1.412	2	1.504	1.455	1.477	0.020
•	$K^{*\prime\prime}$	1^-	$^3S_1/^3\mathbf{D}_1$	1.714	3	1.618	1.588	1.553	0.020
		1^-	$^3\mathbf{S}_1/^3D_1$		4	1.945	1.890	1.852	
•	K_0^*	0^+	$^3P_0$	1.429	1	1.177	1.112	1.115	0.200
		0^+	$^3P_0$		2	1.674	1.587	1.604	
	$K_0^{*\prime}$	0^+	$^3P_0$	1.950	3	2.074	1.989	1.955	
•	K_1	1^+	$^1\mathbf{P}_1/^3P_1$	1.270	1	1.304	1.274	1.288	0.020
•	K_1'	1^+	$^1P_1/^3\mathbf{P}_1$	1.402	2	1.322	1.306	1.321	0.020
	K_1''	1^+	$^1\mathbf{P}_1/^3P_1$	1.650	3	1.773	1.725	1.701	
•	K_2^*	2^+	$^3\mathbf{P}_2/^3F_2$	1.429	1	1.416	1.415	1.415	0.020
	$K_2^{*\prime}$	2^+	$^3\mathbf{P}_2/^3F_2$	1.980	2	1.867	1.849	1.785	
		2^+	$^3P_2/^3\mathbf{F}_2$		3	1.945	1.934	1.831	
	K_2	2^-	$^1\mathbf{D}_2/^3D_2$	1.580	1	1.706	1.693	1.640	
•	K_2'	2^-	$^1D_2/^3\mathbf{D}_2$	1.768	2	1.715	1.711	1.650	0.020
	K_2''	2^-	$^1\mathbf{D}_2/^3D_2$	2.250	3	2.082	2.065	1.962	
•	K_3^*	3^-	$^3\mathbf{D}_3/^3G_3$	1.770	1	1.801	1.813	1.722	0.020
	K_3	3^+	$^1\mathbf{F}_3/^3F_3$	2.320	1	2.027	2.034	1.900	
•	K_4^*	4^+	$^3\mathbf{F}_4/^3H_4$	2.045	1	2.115	2.150	1.967	0.020
	K_4	4^-	$^1G_4/^3\mathbf{G}_4$	2.500	1	2.300	2.333	2.116	
	K_5^*	5^-	$^3G_5/^3\mathbf{I}_5$	2.380	1	2.386	2.449	2.176	
			Charmed mesons: c, u/d quarks						
	Name i	J^{PC}	$^{2s+1}L_J$	$M_i^{\rm expt}$	n	M_i^{Ia}	M_i^{Ib}	M_i^{II}	σ_i
•	D	0^-	$^1S_0$	1.867	1	1.935	1.901	1.904	0.020
•	D^*	1^-	$^3\mathbf{S}_1/^3D_1$	2.010	1	2.006	1.999	2.031	0.020

TABLE III. (*Continued.*)

	Name i	J^{PC}	$^{2s+1}L_J$	$M_i^{\rm expt}$	n	$M_i^{\rm Ia}$	$M_i^{\rm Ib}$	$M_i^{\rm II}$	σ_i
	Charmed mesons: c, u/d quarks								
		0^+	$^3P_0$		1	2.339	2.290	2.264	
•	D_1	1^+	$^1\mathbf{P}_1/^3P_1$	2.424	1	2.406	2.379	2.382	0.020
	$D_J(?)$	1^+	$^1P_1/^3\mathbf{P}_1$	2.440	2	2.439	2.438	2.424	
•	D_2^*	2^+	$^3\mathbf{P}_2/^3F_2$	2.459	1	2.485	2.492	2.484	0.020
	Charmed strange mesons: c, s quarks								
•	D_s	0^-	$^1S_0$	1.969	1	2.032	1.990	1.984	0.020
•	$D_s^*(?)$	1^-	$^3\mathbf{S}_1/^3D_1$	2.110	1	2.100	2.088	2.110	
		0^+	$^3P_0$		1	2.436	2.387	2.349	
•	D_{s1}	1^+	$^1\mathbf{P}_1/^3P_1$	2.537	1	2.498	2.473	2.466	0.020
		1^+	$^1P_1/^3\mathbf{P}_1$		2	2.520	2.516	2.503	
•	$D_{sJ}(?)$	2^+	$^3\mathbf{P}_2/^3F_2$	2.564	1	2.561	2.568	2.563	
	Bottom mesons: b, u/d quarks								
•	B	0^-	$^1S_0$	5.279	1	5.303	5.268	5.247	0.020
•	B^*	1^-	$^3\mathbf{S}_1/^3D_1$	5.325	1	5.336	5.318	5.316	0.020
	Bottomed strange mesons: b, s quarks								
	$B_s(?)$	0^-	$^1S_0$	5.38	1	5.379	5.340	5.317	
	$B_s^*(?)$	1^-	$^3\mathbf{S}_1/^3D_1$	5.43	1	5.413	5.394	5.387	
	Charmonium: c quarks								
•	η_c	0^{-+}	$^1S_0$	2.979	1	3.042	3.010	3.007	0.020
	η_c'	0^{-+}	$^1S_0$	3.590	2	3.615	3.589	3.609	
•	J/Ψ	1^{--}	$^3\mathbf{S}_1/^3D_1$	3.097	1	3.099	3.104	3.117	0.020
•	Ψ'	1^{--}	$^3\mathbf{S}_1/^3D_1$	3.686	2	3.655	3.646	3.665	0.020
•	Ψ''	1^{--}	$^3S_1/^3\mathbf{D}_1$	3.770	3	3.766	3.780	3.775	0.020
•	Ψ'''	1^{--}	$^3\mathbf{S}_1/^3D_1$	4.040	4	4.051	4.017	4.028	0.020
•	Ψ^{iv}	1^{--}	$^3S_1/^3\mathbf{D}_1$	4.159	5	4.124	4.105	4.097	0.020
•	Ψ^{v}	1^{--}	$^3\mathbf{S}_1/^3D_1$	4.415	6	4.376	4.319	4.314	0.020
		1^{--}	$^3S_1/^3\mathbf{D}_1$		7	4.430	4.384	4.364	
•	χ_{c0}	0^{++}	$^3P_0$	3.415	1	3.437	3.433	3.409	0.020
•	χ_{c1}	1^{++}	$^3P_1$	3.511	1	3.485	3.506	3.504	0.020
•	χ_{c2}	2^{++}	$^3\mathbf{P}_2/^3F_2$	3.556	1	3.523	3.562	3.572	0.020
	COG		$^3P_{0,1,2}$	3.525	1	3.501	3.529	3.531	
	h_{c1}	1^{+-}	$^1P_1$	3.526	1	3.492	3.520	3.522	
	Bottonium: b quarks								
	η_b	0^{-+}	$^1S_0$		1	9.454	9.353	9.368	
•	Υ	1^{--}	$^3\mathbf{S}_1/^3D_1$	9.460	1	9.493	9.434	9.441	0.010
•	Υ'	1^{--}	$^3\mathbf{S}_1/^3D_1$	10.023	2	10.011	10.018	10.022	0.010
		1^{--}	$^3S_1/^3\mathbf{D}_1$		3	10.131	10.171	10.160	
•	Υ''	1^{--}	$^3\mathbf{S}_1/^3D_1$	10.355	4	10.346	10.348	10.365	0.010
		1^{--}	$^3S_1/^3\mathbf{D}_1$		5	10.423	10.444	10.451	
•	Υ'''	1^{--}	$^3\mathbf{S}_1/^3D_1$	10.580	6	10.614	10.599	10.626	0.010
		1^{--}	$^3S_1/^3\mathbf{D}_1$		7	10.672	10.670	10.688	
•	Υ^{iv}	1^{--}	$^3\mathbf{S}_1/^3D_1$	10.865	8	10.846	10.811	10.844	0.010
		1^{--}	$^3S_1/^3\mathbf{D}_1$		9	10.893	10.868	10.892	
•	Υ^{v}	1^{--}	$^3\mathbf{S}_1/^3D_1$	11.019	10	11.054	11.000	11.035	0.010
•	χ_{b0}	0^{++}	$^3P_0$	9.860	1	9.859	9.863	9.843	0.010
•	χ_{b0}	0^{++}	$^3P_0$	10.232	2	10.220	10.229	10.232	0.010
•	χ_{b1}	1^{++}	$^3P_1$	9.892	1	9.882	9.906	9.888	0.010
•	χ_{b1}	1^{++}	$^3P_1$	10.255	2	10.239	10.258	10.261	0.010
•	χ_{b2}	2^{++}	$^3\mathbf{P}_2/^3F_2$	9.913	1	9.901	9.938	9.922	0.010
•	χ_{b2}	2^{++}	$^3\mathbf{P}_2/^3F_2$	10.268	2	10.253	10.281	10.284	0.010
	COG		$^3P_{0,1,2}$	9.900	1	9.890	9.919	9.902	
	COG		$^3P_{0,1,2}$	10.260	2	10.245	10.267	10.271	

improve, however.

In case II the modified Richardson potential V_M in combination with a mixed scalar-vector $V_{\rm con}$ was taken. The value $\alpha_0 = 16\pi/27$ was the only parameter held fixed, so that eight parameters were varied. In spite of the extra parameter, the resulting fit (II), see Tables II and III, is worse than the fits found for case I and gave $\chi^2 = 322$.

VI. DISCUSSION

The meson spectrum calculated for parameter sets Ia, Ib, and II is given in Table III. Also the mesons that were not involved in the fitting procedure (the ones without a σ) were calculated. It is seen that most of these unconfirmed mesons (see [24]), are reasonably well described by the model. Many states are a mixture between two $^{2s+1}L_J$ waves. Only in the NR limit these waves decouple because only then the angular momentum l is a good quantum number (see Sec. II C). For each state the most dominant wave is in bold. Most distributions are like 99% vs 1%, which supports the statement that l is almost a good quantum number.

A few years ago (for a review, see page VII of [24]), $\rho(1450)$ and $\rho(1700)$ were recognized as being a splitting in the formerly known $\rho(1600)$ resonance. It could be interpretated as the fine-structure splitting between the $n = 2$, dominantly S states and the $n = 3$, dominantly D states. The splitting however is rather big (~ 250 MeV). For the present model this interpretation was found to be in conflict with the rest of the spectrum. A correct $\rho' - \rho''$ splitting induced a far too large splitting in the 1^{--} states of charmonium and bottonium, and vice versa. Only if the ρ' was regarded to consist of the $n = 2$ and $n = 3$ states, and the ρ'' of the $n = 4$ and $n = 5$ states, correct splittings for the entire spectrum could be obtained. In addition, the correct splitting between the observed ρ''' and ρ^{iv} (~ 50 MeV) was obtained. The difference between the $n = 2$ and $n = 3$ mass, and between the $n = 4$ and $n = 5$ mass, was found to be $\sim$ 100 MeV, which is much smaller than the decay widths of the ρ' and the ρ'' (~ 300 MeV).

In the fits discussed so far the a_0 was regarded as an established meson. However, there are indications that the a_0 is not a $q\bar{q}$ system, but a $K\overline{K}$ molecule. In that case not the a_0 but the a_0' would be the lowest radial excitation of the $J^{PC} = 0^{++}$ channel. Therefore also fits in which the a_0 was not regarded and fits in which the a_0' was identified with the lowest 0^{++} excitation were made. It appeared, however, that there was a preference of the lowest 0^{++} excitation, to lie around 1 GeV, i.e., the mass of the a_0. The identification of the a_0' with the lowest excitations led to considerably worse fits. These results indicate that in the light of the present quark model the a_0 *is* to be regarded as a $q\bar{q}$ state and *not* as a $K\overline{K}$ molecule.

The masses of the π, K, and K_0^* are found to be much too large. As was already mentioned, this was to be expected, because the small masses of these particles are believed to be a consequence of spontaneous breaking of chiral symmetry. In all cases Ia, Ib, and II, the mass of the η_c is found to be too high. As was pointed out by Hirano *et al.* [26], this is probably a consequence of the omission of negative energy states. They found that for a quark model based on the instantaneous ladder Bethe-Salpeter equation for charmonium, the η_c is strongly influenced by neglecting these states (~ 100 MeV), while the influence on all other states is much weaker (~ 10 MeV). If one extrapolates these results to the present theory, this means that the omission of the negative-energy states only weakly affects the spectrum. Only for the $^1S_0$ ground states may a substantial mass drop occur. This would mean that also the masses of the D and the D_S, which are now found a bit too high, would become smaller. The B would also get a smaller mass, which only has a positive result in case Ia.

The center-of-gravity COG(n) (see, e.g., Sec. 8.1 of [1]) is defined by

$$\mathrm{COG}(n) \equiv \frac{5}{9}M(n^3P_2) + \frac{1}{3}M(n^3P_1) + \frac{1}{9}M(n^3P_0).$$

It can be proved that, for an arbitrary scalar potential V_S and a Coulomb vector potential V_V, up to first-order relativistic corrections, this COG equals the corresponding n^1P_1 singlet. The relation is violated by the Q dependence of α_s and the presence of a confining term in the vector direction. It is also affected by higher-order relativistic corrections. In all cases the COG is found to be somewhat higher than the corresponding singlet state. A related quantity is the ratio [1,27]

$$\rho = \frac{M(^3P_2) - M(^3P_1)}{M(^3P_1) - M(^3P_0)}. \tag{6.1}$$

Its experimental value is 0.21 for $u\overline{du}\overline{d}$, 0.48 for $c\bar{c}$, 0.66 for $n = 1$ $b\bar{b}$, and 0.57 for $n = 2$ $b\bar{b}$. For all three cases Ia, Ib, and II, a rather constant value of $\rho \sim 0.8$ (see Table II) was found. A perturbative configuration space calculation shows (see, e.g., Sec. 4.2 of [1]) that this too large value for ρ is a consequence of the dominance of the vector OGE. An analysis for the present case in momentum space gives a similar result. One can also prove that $\rho = 2$ for an arbitrary purely scalar potential. The splittings $M(^3P_2) - M(^3P_1)$ and $M(^3P_1) - M(^3P_0)$, however, then both have the wrong sign. From this it follows that the value of ρ must be very sensitive to the competition between the vector Coulomb part and the scalar part of the potential. This is so because the path from the one extreme to the other involves the change of sign of both splittings. This in addition explains why the experimental value of ρ differs so much for the different quarkonia, because the competition between the vector Coulomb and the scalar potential depends on the relevant momentum scale.

The following remarks on the parameter sets can be made. From Table II it is seen that the quark masses are substantially larger than usual in quark models. Furthermore, the masses are quite different for the different cases. The smallest masses are obtained by fit Ia. This is a consequence of the large negative constant $C \sim -1.0$ GeV, which, however, is necessary in order

to obtain a good fit for the entire spectrum. If, for instance, one only considers bottonium and charmonium, it turns out that the quality of the fit only weakly depends on the value of C. The system is overparametrized and one in fact does not even need a constant in the potential. But, when simultaneously also good results for the lighter mesons are required, the large negative constant arises automatically.

The total string tension $\lambda_{\rm tot}$ is defined as the sum of the tensions in vector and scalar direction. For case I one has $\lambda_{\rm tot} = \lambda + \frac{1}{2}\alpha_0\Lambda^2$, while case II simply gives $\lambda_{\rm tot} = \lambda$. These tensions are also quite different for the different cases. In case Ib, which gave the best fit, there is only a vector tension. This is in contrast to the requirement that, in order to obtain better ρ values, the confining should be dominantly scalar. The total tension for case Ia is closest to the value $\lambda \sim 0.18$ GeV^2, which is often given in the literature.

The Regge slopes of Ia and Ib are compatible with the experimental value $\beta \approx 1.2$ GeV^2. The slope found in II is somewhat too low. This can clearly be seen from the high-J states like the ρ_5, a_6, and K_5^*. The errors given in Table II represent a measure of linearity of the trajectories. It is defined as the spread in the difference between the masses squared of adjacent states. The spreads found are considerably smaller than the experimental value.

Finally the running coupling constant for $Q = 31$ GeV and for Q equal to the mass of the weak Z boson ($Q = M_Z = 91.16$ GeV) were compared with the experimental values

$$\alpha_s(34\ \text{GeV}) = 0.14 \pm 0.02,$$
$$\alpha_s(M_Z) = 0.1134 \pm 0.0035.$$

Only case Ia is compatible with both conditions. The choice $\alpha_0 = 1.75$ was made to give the best approximation to the QCD formula, Eq. (3.4), for moderate momentum transfer. Now it appears that this choice also gives correct results for very high momenta. A fit of type Ia, but now with $\alpha_0 = 16\pi/27$ (not displayed) gave a too large high momentum α_s. In principle, the high Q range of the potential is completely irrelevant for the calculation of the meson spectrum, where the potential is only tested up to a few GeV. Nevertheless, for the sake of theoretical consistency, this test was made.

VII. CONCLUDING REMARKS

In this paper a relativistic quark model defined in momentum space was studied. The quark-antiquark potential used consisted of a OGE with a Lorentz vector character and a linear plus constant confining potential. For the OGE the Richardson potential V_R, given by Eq. (3.6), with and without its linear part, as well as a modified Richardson potential V_M, defined by Eq. (3.7), was regarded. Best results were obtained for the Richardson potential including its linear term (case I). The linear plus constant potential was given a pure scalar character, i.e., $\epsilon = 0$ in Eq. (2.6). In this way, the confining in the vector direction was induced by the linear part of V_R. For case I two different fits were made, fit Ia, in which the value of α_0 was fixed to 1.75, and fit Ib, in which α_0 was varied, but the string tension in the scalar direction λ was put equal to zero. Also reasonable well results were obtained for $V_{\rm OGE} = V_R$ (case II). Here the confining potential was given a mixed scalar-vector character. For the fits Ia, Ib, and II, most meson masses, with the exception of π, K, and K_0^* were found to be reasonably described by the model. In cases Ia and Ib correct Regge slopes were found, and only in case Ia a correct strong coupling constant for large momenta was found. The ratios ρ, defined by Eq. (6.1), however, were in all three cases found to be too large. It is concluded that case Ia should be preferred.

No detailed comparison with other theories has been made because the main purpose of the present application was not so much to improve upon the existing calculations, but rather to show that results of the same quality could be obtained using a relativistic theory which is formulated in the momentum representation.

APPENDIX A: PARTIAL-WAVE DECOMPOSITION

In this appendix we give the precise form of the decomposition of a potential W defined by Eq. (2.6). The partial-wave potentials

$$V_{ij}^{nJ} = (V_V)_{ij}^{nJ} + (V_S)_{ij}^{nJ}, \quad n = s,t,$$

defined by Eq. (2.10) can in general be expressed in terms of the "spinless" partial waves W_V^l and W_S^l of V_V and V_S, respectively. They are defined by

$$W_{V,S}^l(p',p) = (2\pi p'p)R(p',p)\int_{-1}^{+1} W_{V,S}(\mathbf{p}',\mathbf{p})P_l(x)dx, \tag{A1}$$

with $x = \frac{\mathbf{p}'\cdot\mathbf{p}}{p'p}$ and P_l the Legendre polynomial of order l. The quantity R is defined by $R(p',p) = A_1'A_2'A_1A_2$, with $A = \sqrt{\frac{E+m}{2E}}$. If furthermore $b = \frac{p}{E+m}$, then the result is the following: Vector potential for the $|s_{1,2}\rangle$ states

$$(V_V)_{11}^{sJ}(p',p) = [1 + 3(b_1'b_2' + b_1b_2) + b_1'b_2'b_1b_2]\,W_V^J + (b_1' - b_2')(b_1 - b_2)\frac{(J+1)W_V^{J+1} + JW_V^{J-1}}{2J+1},$$
$$(V_V)_{12}^{sJ}(p',p) = (b_2' - b_1')(b_2 + b_1)\sqrt{J(J+1)}\frac{W_V^{J+1} - W_V^{J-1}}{2J+1} = (V_V)_{21}^{sJ}(p,p'), \tag{A2}$$
$$(V_V)_{22}^{sJ}(p',p) = (1 + b_1'b_2')(1 + b_1b_2)W_V^J + (b_1' + b_2')(b_1 + b_2)\frac{JW_V^{J+1} + (J+1)W_V^{J-1}}{2J+1}.$$

Vector potential for the $|t_{1,2}\rangle$ states

$$
\begin{aligned}
(V_V)^{tJ}_{11}(p',p) &= (1-b_1'b_2')(1-b_1b_2)\frac{(J+1)W_V^{J+1}+JW_V^{J-1}}{2J+1}+[(b_1'-b_2')(b_1-b_2)+4(b_1'b_2+b_2'b_1)]\,W_V^J,\\
(V_V)^{tJ}_{12}(p',p) &= -(1-b_1'b_2')(1+b_1b_2)\sqrt{J(J+1)}\frac{W_V^{J+1}-W_V^{J-1}}{2J+1}=(V_V)^{tJ}_{21}(p,p'),\\
(V_V)^{tJ}_{22}(p',p) &= (1+b_1'b_2')(1+b_1b_2)\frac{JW_V^{J+1}+(J+1)W_V^{J-1}}{2J+1}+(b_1'+b_2')(b_1+b_2)W_V^J.
\end{aligned}
\tag{A3}
$$

Scalar potential for the $|s_{1,2}\rangle$ states

$$
\begin{aligned}
(V_S)^{sJ}_{11}(p',p) &= (1+b_1'b_2'b_1b_2)W_S^J-(b_1'b_1+b_2'b_2)\frac{(J+1)W_S^{J+1}+JW_S^{J-1}}{2J+1},\\
(V_S)^{sJ}_{12}(p',p) &= (b_1'b_1-b_2'b_2)\sqrt{J(J+1)}\frac{W_S^{J+1}-W_S^{J-1}}{2J+1}=(V_S)^{sJ}_{21}(p,p'),\\
(V_S)^{sJ}_{22}(p',p) &= (1+b_1'b_2'b_1b_2)W_S^J-(b_1'b_1+b_2'b_2)\frac{JW_S^{J+1}+(J+1)W_S^{J-1}}{2J+1}.
\end{aligned}
\tag{A4}
$$

Scalar potential for the $|t_{1,2}\rangle$ states

$$
\begin{aligned}
(V_S)^{tJ}_{11}(p',p) &= (1+b_1'b_2'b_1b_2)\frac{(J+1)W_S^{J+1}+JW_S^{J-1}}{2J+1}-(b_1'b_1+b_2'b_2)W_S^J,\\
(V_S)^{tJ}_{12}(p',p) &= -(1-b_1'b_2'b_1b_2)\sqrt{J(J+1)}\frac{W_S^{J+1}-W_S^{J-1}}{2J+1}=(V_S)^{tJ}_{21}(p,p'),\\
(V_S)^{tJ}_{22}(p',p) &= (1+b_1'b_2'b_1b_2)\frac{JW_S^{J+1}+(J+1)W_S^{J-1}}{2J+1}-(b_1'b_1+b_2'b_2)W_S^J.
\end{aligned}
\tag{A5}
$$

Strictly speaking, these results are only valid for $J>0$. For $J=0$ only the V_{11}'s are nonzero and are also given by Eqs. (A2)–(A5), but with $W^{l=-1}=0$.

In the equal-mass case there is no difference between the b_1's and the b_2's. From this it is seen that the V_{12}^{sJ}'s and the V_{21}^{sJ}'s are zero. This means that the potential decouples with regard to the $|s_1\rangle$ state, which corresponds to the $l=J$ singlet, and the $|s_2\rangle$ state, which corresponds to the $l=J$ triplet. Therefore in this case only the $|l=J\pm1\rangle$ triplet states mix. In the unequal-mass case the $l=J$ singlet and triplet states mix.

APPENDIX B: SPINLESS DECOMPOSITION OF THE RICHARDSON POTENTIALS V_R AND V_M

In this appendix the spinless partial-wave decompositions W_R and W_M of the potentials V_R and V_M, defined by Eqs. (3.6) and (3.7) will be calculated.

The momentum transfer Q^2 which is defined by Eq. (3.2) depends on the lengths $p=|\mathbf{p}|$ and $p'=|\mathbf{p}'|$ of the incoming and outgoing momentum, and on the angle $x=\frac{\mathbf{p}\cdot\mathbf{p}'}{pp'}$ between these two momenta:

$$
Q^2=Q^2(p,p',x)=2pp'(z_0-x). \tag{B1}
$$

Here

$$
z_0(p,p')=\frac{p^2+p'^2-\tau(p,p')}{2pp'}, \tag{B2}
$$

where the retardation τ is a theory dependent quantity which in the present case is given by Eq. (2.3). The spinless partial wave $W^l(p',p)$ corresponding to an angular momentum l is defined by Eq. (A1). Introducing

$$
y(x)=1+\frac{Q^2(x)}{\Lambda^2},\quad b=\frac{\Lambda^2}{2pp'} \tag{B3}
$$

and $y_\pm=y(x=\mp1)\geq1$, then W_R^l and W_M^l are given by

$$
W_R^l=-\frac{\alpha_0 R}{2\pi}\int_{y_-}^{y_+}\frac{P_l[z_0-b(y-1)]}{(y-1)\ln y}dy, \tag{B4}
$$

$$
W_M^l=-\frac{\alpha_0 R}{2\pi}\int_{y_-}^{y_+}\frac{P_l[z_0-b(y-1)]}{y\ln y}dy. \tag{B5}
$$

The y dependence in P_l can be expanded, by using

$$
P_l(z-w)=\sum_{i=0}^{l}g_i^l(z)w^i. \tag{B6}
$$

Here g_i^l is a polynomial of degree $l-i$. For $l\leq3$ it is given in Table IV. For general l it can be found from the recurrence relation

$$
(l+1)g_i^{l+1}=(2l+1)(zg_i^l-g_{i-1}^l)-lg_i^{l-1}, \tag{B7}
$$

in combination with the initial values

$$
g_0^{-1}(z)=0,\quad g_0^0(z)=1. \tag{B8}
$$

TABLE IV. The polynomials g_i^l for $l \leq 3$, defined by (B6).

$l \setminus i$	0	1	2	3
0	1			
1	z	-1		
2	$\frac{3}{2}z^2 - \frac{1}{2}$	$-3z$	$\frac{3}{2}$	
3	$\frac{5}{2}z^3 - \frac{3}{2}z$	$-\frac{15}{2}z^2 + \frac{3}{2}$	$\frac{15}{2}z$	$-\frac{5}{2}$

Note that g_0^l obeys the recurrence relation of the Legendre polynomials. In combination with the initial values, Eq. (B8), it follows that $g_0^l = P_l$.

The partial waves W_R^l and W_M^l can be written in terms of g_i^l's and the integrals

$$A_n = \frac{b^n}{2}\int_{y_-}^{y_+} \frac{(y-1)^n}{y \ln y} dy, \quad n \geq -1. \tag{B9}$$

For $n = -1$ one has

$$A_{-1} = \frac{1}{2b}\left[F(\ln y_+) - F(\ln y_-)\right], \tag{B10}$$

where

$$F(x) \equiv -\int_x^\infty \frac{dt}{t(e^t - 1)}, \quad x > 0. \tag{B11}$$

For $n \geq 0$ the integrals A_n can be expanded into

$$A_n = \frac{b^n}{2}\sum_{k=0}^{n} \binom{n}{k} (-1)^{(n-k)} I_k, \tag{B12}$$

where

$$I_n = \int_{y_-}^{y_+} \frac{y^{n-1}}{\ln y} dy, \; n \geq 0. \tag{B13}$$

One finds

$$I_0 = \ln\left[\frac{\ln y_+}{\ln y_-}\right], \tag{B14}$$

$$I_n = Ei(n \ln y_+) - Ei(n \ln y_-), \quad n > 0, \tag{B15}$$

where

$$Ei(x) \equiv \fint_{-\infty}^{x} \frac{e^t}{t} dt \tag{B16}$$

is the exponential integral (see (5.1.2) of [22]). The principal-value integral is denoted by $\fint$.

Summarizing all steps it follows that W_R^l and W_M^l, defined by Eqs. (A1), (3.6) and (3.7), are given by

$$W_R^l(p,p') = -\frac{\alpha_0 R}{\pi}\sum_{i=0}^{l} g_i^l(z_0)(A_i + bA_{i-1}), \tag{B17}$$

$$W_M^l(p,p') = -\frac{\alpha_0 R}{\pi}\sum_{i=0}^{l} g_i^l(z_0) A_i, \tag{B18}$$

where the polynomials g_i^l are defined by Eq. (B6) and the integrals A_n can be found from Eqs. (B10) and (B12).

[1] W. Lucha, F. Schöber, and D. Gromes, Phys. Rep. **200**, 127 (1991).
[2] D. Eyre and J.P. Vary, Phys. Rev. D **34**, 3467 (1986).
[3] W.D. Heiss and G.M. Welke, J. Math. Phys. **27**, 936 (1986).
[4] F. Gross and J. Milana, Phys. Rev. D **43**, 2401 (1991).
[5] J.W. Norbury, D.E. Kahana, and K.M. Maung, Can. J. Phys. **70**, 86 (1992).
[6] K.M. Maung, D.E. Kahana, and J.W. Norbury, Phys. Rev. D **47**, 1182 (1993).
[7] H. Hersbach, Phys. Rev. D **47**, 3027 (1993).
[8] H. Hersbach, Phys. Rev. A **46**, 3657 (1992).
[9] P.A.M. Dirac, Rev. Mod. Phys. **21**, 392 (1949).
[10] M.G. Olsson and K.J. Miller, Phys. Rev. D **28**, 674 (1983).
[11] M. Jacob and G.C. Wick, Ann. Phys. (N.Y.) **7**, 404 (1959).
[12] H. Hersbach and Th.W. Ruijgrok, Z. Phys. D **18**, 209 (1991).
[13] H.A. Bethe and E.E. Salpeter, *Quantum Mechanics of One- and Two-electron Atoms* (Plenum Publishing Corporation, New York, 1977).
[14] J.L. Richardson, Phys. Lett. **82B**, 272 (1979).
[15] J.L. Basdevant and S. Boukraa, Z. Phys. C **28**, 413 (1985).
[16] A. Martin, Z. Phys. C **32**, 359 (1986).
[17] P.C. Tiemeijer and J.A. Tjon, Phys. Rev. C **49**, 494 (1994).
[18] P.C. Tiemeijer, Ph.D. thesis, 1993 (unpublished).
[19] P.C. Tiemeijer and J.A. Tjon, Phys. Rev. C **48**, 896 (1993).
[20] G.L. Payne, *Proceedings of Models and Methods in Few-Body Physics, Lisboa, Portugal* (Springer-Verlag, Berlin, 1986), p. 273; H. Kröger, R.J. Slobodrian, and G.L. Payne, Phys. Rev. C **28**, 607 (1983).
[21] J. Sloan, Comput. Phys. **3**, 322 (1968).
[22] M. Abramowitz and A. Stegun, *Handbook of Mathematical Functions* (Dover Publications, New York, 1972).
[23] W.H. Press, B.P. Flannery, S.A. Teukolski, and W.T. Vetterling, *Numerical Recipes in C*, 2nd ed. (Cambridge University Press, Cambridge, 1992).
[24] Particle Data Group, K. Hikasa *et al.*, Phys. Rev. D **45**, Part 2 (1993). For a summary, see *Particle Properties Data Booklet* (American Institute of Physics, New York, 1992).
[25] H.W. Crater and P. Van Alstine, Phys. Rev. Lett. **53**, 1527 (1984); Phys. Rev. D **36**, 3007 (1987); **37**, 1982 (1988); Nucl. Phys. B (Proc. Suppl.) **6**, 271 (1989).
[26] M. Hirano, K. Iwata, K. Kato, T. Murota, and D. Tsuruda, Prog. Theor. Phys. **69**, 1498 (1983).
[27] H.J. Schnitzer, Phys. Rev. Lett. **35**, 1540 (1975).
[28] E760 Collaboration, T.A. Armstrong *et al.*, Phys. Rev. Lett. **69**, 2337 (1992).